Batteries & Supercaps

Supporting Information

Enhanced Electrochemical Performance of NTP/C with Rutile TiO_2 Coating, as Anode Material for Sodium-Ion Batteries

Teja Stüwe, Daniel Werner, David Stock, Christoph W. Thurner, Alexander Thöny, Christoph Grießer, Thomas Loerting, and Engelbert Portenkirchner*

1. Experimental

1.1 Material Synthesis

NTP and NTP-RT Synthesis

NTP and NTP-RT synthesis was carried out after the procedure of Yang et al. [35].

$NaH_2PO_4 \cdot 2H_2O + 2TiO_2 + 2\ H_3PO_4 \rightarrow NaTi_2(PO_4)_3 + 6H_2O$

For NTP and NTP-RT 1.5 mL $NaH_2PO_4 \cdot 2\ H_2O$, 1.5 mL 85 wt.-% H_3PO_4 aqueous solution, 1.5 mL deionized water and 1.5 g anatase TiO_2 nanopowder were mixed and creamed well in a mortar.
Then the mixture was collected and transferred to a stainless steel hydrothermal autoclave with Teflon liner (50 mL cylinder volume) and heated in an oven at 180 °C for 72 h. For NTP-RT the synthesis was performed with a reaction time of 6 h and reaction temperature of 150 °C.
After cooling to room temperature, the obtained white precipitate was purified with deionized water and ethanol by centrifugation, three times subsequently. To yield the final product the white residual was collected and dried at 60 °C over night. For NTP and NTP-RT, a white powder with a yield of 85% and 68% could be obtained, respectively.
XRD and SEM measurements were performed for a structural and morphological characterization. XRD, Raman and XPS measurements were conducted to identify successful rutile TiO_2 coating.

NTP/C and NTP/C-RT Synthesis

According to Yang et al. [1] the as synthesized NTP was used for the preparation of carbon coated NTP nanopowder. 0.5 g NTP was mixed with 10 mL of a 10% glucose (Alfa Aesar, 99%) solution.
For the preparation of NTP/C-RT, 1.3 g NTP-RT was mixed with 23 mL of a 10% glucose solution. The mixture was dried at 60 °C over night.

$C_6H_{12}O_6 \rightarrow 6C + 6H_2O$

The mixture was ground to fine powder in a porcelain mortar and heated at 600 °C for 4 h under Ar atmosphere (heating rate of 5 °C/min, Ar-flow of 150 sccm). The product was then grounded to fine powder and used for electrode fabrication.
SEM images were taken for morphological characterization. Raman spectroscopy was performed to analyze the carbon layer. TGA analysis was used to determine the carbon content.

Electrode Fabrication

All electrodes were prepared using a copper foil (Mateck, thickness 0.1 mm) as current collector, which was roughened with sandpaper for better adherence. Round discs were punched out with a diameter of d = 17 mm. The electrodes were flattened using a hydraulic press with about one ton per 2.27 cm^2. The relevant active material was mixed with carbon black (CABOT, VXC 72) as conductive material and PTFE (Sigma Aldrich) as a binder in a weight ratio of 70:20:10. Water or ethanol was mixed with the remaining components to obtain a slurry which can then be applied on the copper foil. For the carbon coated samples the carbon content was substracted to calculate the active mass per area values. After applying the slurry the electrode was dried over night at 60 °C. The active material areal loading for NTP, NTP-RT, NTP/C and NTP/C-RT was 7, 7, 6 and 3 mg/cm^2, respectively.

Battery Assembly

For electrochemical characterization with an organic electrolyte, ECC-Ref cells from EL-CELL were used as test battery cell. A half-cell, three-electrode cell setup was chosen, where the working electrode (WE) consists of the electrodes, metallic sodium (Na rods in paraffin oil, VWR, 99.5%) is used as counter electrode (CE) and reference electrode (RE). The cells were assembled in an Ar filled glovebox (UNI-lab, MBRAUN). Na for the RE was loaded using a reference loading tool (ECC-REFLOAD). Glass fibre was used as a separator (d = 18 mm, thickness 1.55 mm, EL-Cell). The separator was soaked with 500 µl of a Na containing organic electrolyte, 1 M NaFSI (sodium bis(fluorosulfonyl)imide) in ethylene carbonate (EC) and dimethylcarbonate electrolyte (DMC) (EC:DMC 1:1 v/v, SOLVIONIC, 99.9%).

1.2 Electrochemical Characterization

ECC-Ref Cell (ELCELL) test batteries for measurements in organic electrolyte. Electrochemical measurements were carried out for all setups using a BIOLOGIC VMP3 potentiostat and the EC-LAB V10.44 software. Electrochemical measurements for the performance of the electrode material included open circuit voltage (OCV), potentiostatic electrochemical impedance spectroscopy (PEIS), cyclic voltammetry (CV) and galvanostatic cycling with potential limits (GCPL).
OCV and PEIS were measured prior and after each CV scan. Always 5 cycles were scanned for each CV. CV currents were referenced to the geometric electrode area of 2.27 mA/cm^2 and are therefore given in mA/cm^2. The GCPL measurements in an organic electrolyte were performed for NTP, NTP/C, NTP-RT and NTP/C-RT at different C-rates in a constant potential window between 3.0 and 1.0 V vs. Na^+/Na. The theoretical capacity of NTP is 133 mAh/g. In the following sequence 15 cycles at 0.1 C, 0.5 C, 1 C, 0.5 C and 40 cycles at 0.1 were measured.

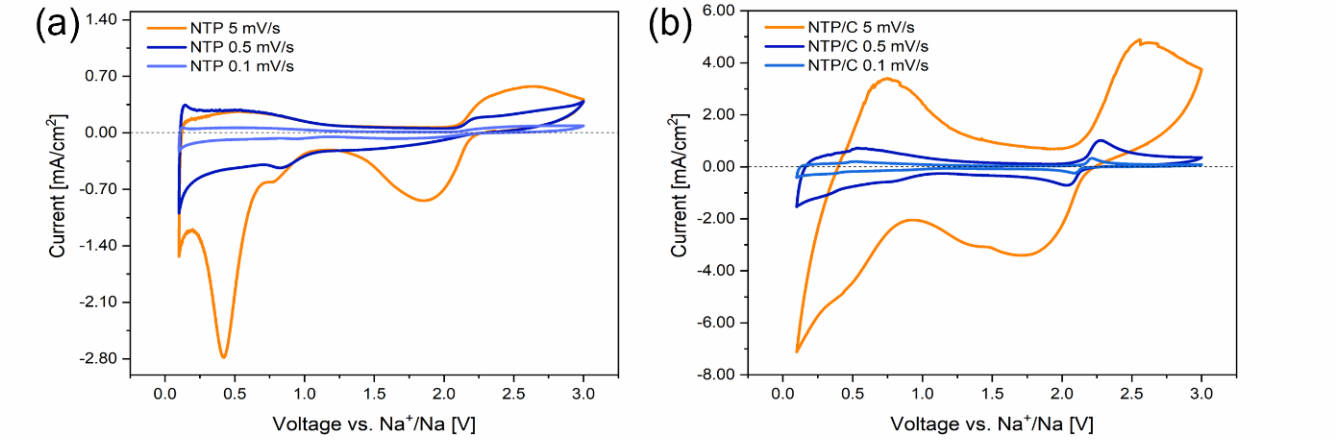

Figure S1: Cyclo-voltammogram of a) NTP and b) NTP/C at scan rates of 5, 0.5 and 0.1 mV/s.

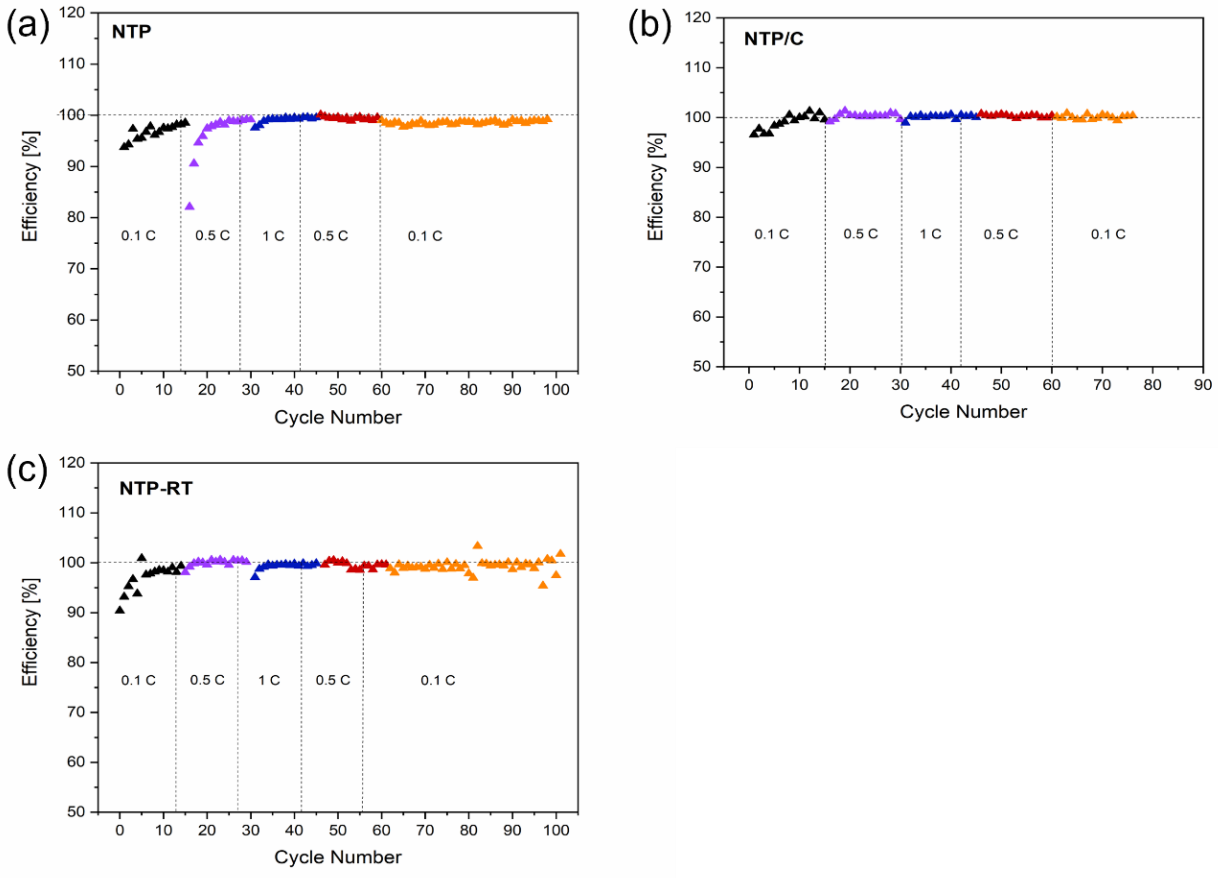

Figure *S2*: Coulombic efficiencies for a) NTP, b) NTP/C and c) NTP-RT.

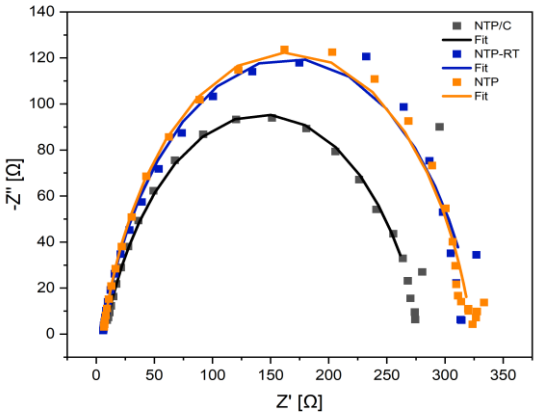

Figure S3: Nyquist plots and corresponding fits for NTP/C, NTP-RT and NTP.

Table S1: Ohmic resistance and charge transfer resistance values for NTP/C, NTP-RT and NTP

	R_Ω [Ω/mg]	R_{ct} [Ω/mg]
NTP/C	0.28	8.2
NTP-RT	0.35	19
NTP	0.65	30

The ohmic resistance (R_Ω) representing the resistance of the electrolyte and the charge transfer resistance (R_{ct}) was determined for NTP/C, NTP-RT and NTP using impedance measurements. The calculated resistance was related to the mass of the electrode material as it significantly influences the resistance values.

1.3 Material characterization

Scanning Electron Microscopy (SEM)

SEM images of NTP, NTP-RT, NTP/C and NTP/C-RT were taken. SEM imaging was performed with a JEOL JSM-7601F field emission electron microscope. With an acceleration voltage of 10 kV and a secondary electron imaging detector. The magnifications of 20000x, 10000x, 5000x and 1000x were applied.

Powder X-ray Diffraction (XRD)

XRD measurements were carried out for NTP and NTP-RT. The powder X-ray diffraction patterns were recorded at ambient temperature with a Stoe Stadi P powder diffractometer in Debye−Scherrer geometry. The instrument was operated with Mo K1 radiation [λ= 0.7093 Å, Ge(111) monochromator] and a Mythen 2 DCS4 detector. Evaluations of the powder X-ray diffraction patterns were carried out with the WinXPOW 3.07 software package. The structure analysis is based on the references from the Crystallography Open Database (COD) using the Fullprof software tool.
A XRD pattern comparison between NTP and NTP-RT is shown in **Figure S3b**, to identify the existence of rutile TiO_2 coating. It appears that the structures are almost identical to each other. 12.5° a small peak is visible in the NTP-RT XRD pattern which can be assigned to rutile TiO_2. This peak can not be seen in the NTP pattern.
In theory, due to the shorter reaction time and temperature the TiO_2 precursor cannot completely react with the other starting materials and be converted to NTP and subsequently gets adsorbed on the NTP nanocube surface as TiO_2 layer. Due to the combination of elevated temperature, and pressure in the autoclave reaction vessel the anatase TiO_2 undergoes a phase transition into rutile TiO_2. Consequently, no peaks are visible in the NTP and NTP-RT XRD pattern which can be attributed to anatase TiO_2. Due to many overlapping peaks of NTP and rutile TiO_2 and the small fraction of TiO_2 coating compared to NTP, Raman spectra and XPS analysis for further characterization of the rutile TiO_2 layer were performed

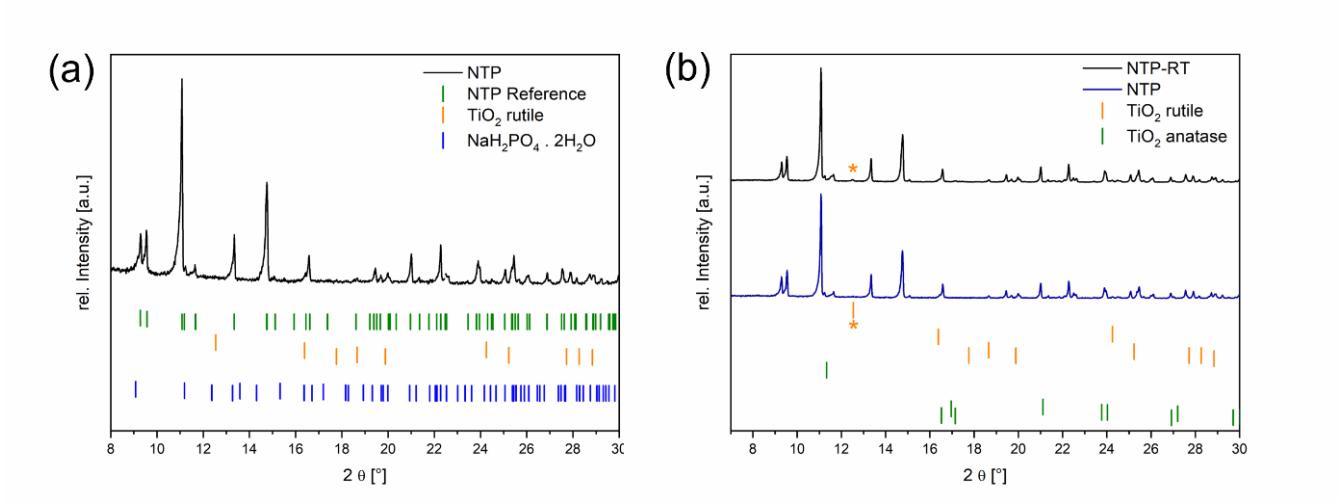

Figure *S4*: Powder XRD diffractogram of a) NTP, NTP-RT and b) NTP with reference reflex positions.

Raman Spectroscopy

Raman spectra were taken using a WITec Confocal alpha 300 R Raman Imaging Microscope, including a laser of a wavelength of 532 nm and a maximal power output of 20 mW, with a ZEISS LD Plan-NEOFLUAR/40×-objective. The spectra were collected using an 600 g/mm grating and a charged coupled device (CCD)-camera. The relative intensities of D and G-band of graphite were calculated using following equation:

CE =I(D)/ I(G)

Where I(D) is the intensity of the D-band and I(G) stands for the intensity of the G-band.

In **Figure S4a** two broad bands visible in the carbon coated sample at 1340 and 1591 cm^{-1}. These two peaks can be attributed to the D- and G-band of graphite. The relative intensity of D and G-band were calculated with and 0.59, this indicates an amorphous structure of carbon.
Reference Raman peaks for rutile TiO_2 are shown in **Figure S4b** (orange bars) [38]. The characteristic stretching peaks for rutile TiO_2 are located at 140, 430 and 590 cm^{-1}. NTP-RT (blue curve) shows a high relative intensity for the peak at 140 cm^{-1} and an additional shoulder at 430 cm cm^{-1}. This could be a sign for the existence of a rutile TiO_2 layer.
The peak shift visible in **Figure S5c** has already been reported in literature and can be explained with a blurred separation between active Raman shifts and silent modes. This can be because of a different environment which changes the polarization. [37,39]

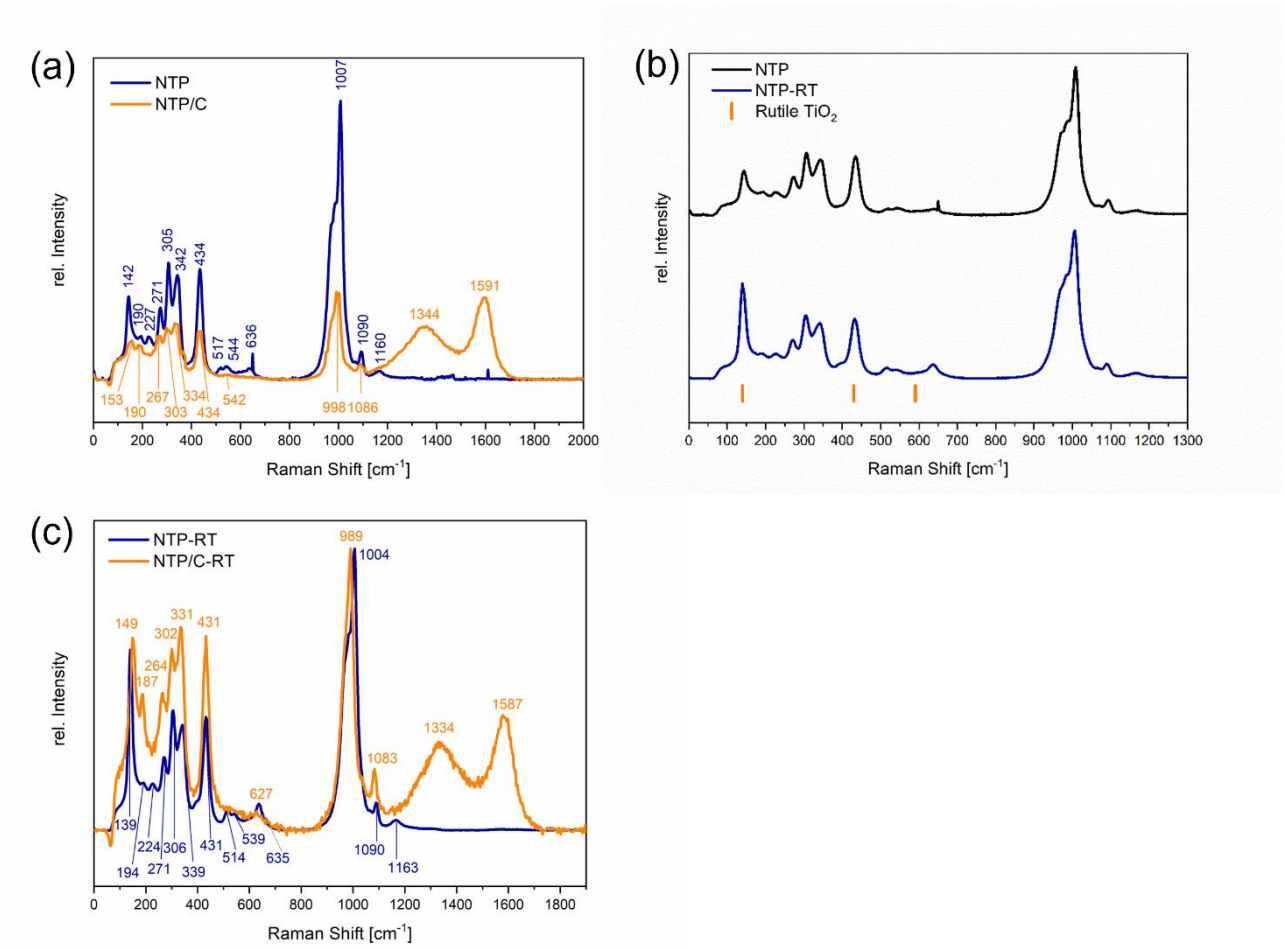

Figure S5: Raman spectra of a) NTP and NTP/C, b) NTP and NTP-RT with reference positions of rutile TiO2, c) NTP-RT and NTP/C-RT in the range from 0 to 2000 cm^{-1}.

Table S2: NTP Raman Peaks and corresponding chemical bond vibration.

NTP **Raman shift [cm^{-1}]**	**NTP/C** **Raman shift [cm^{-1}]**	**NTP-RT** **Raman shift [cm^{-1}]**	**NTP/C-RT** **Raman shift [cm^{-1}]**	**Assigned peaks**
142, 190, 271	153, 190, 267	139, 194, 271	149, 187, 264	Ti^{4+} phonon
227, 517		224, 396, 514	-	Ti^{4+} phonon – overtone
305, 342, 434	303, 334, 434	306, 339, 431	302, 331, 431	PO_4^{3-} phonon
544, 636	542	539, 635	627	PO_4^{3-} phonon – overtone
1007	998	1004	989	ν_1 symmetric stretching vibration of PO_4^{3-}
1090	1086	1090	1083	ν_3 asymmetric stretching vibration of PO_4^{3-}
1160	-	1163	-	ν_s P=O
-	1344	-	1334	D-band
-	1591	-	1587	G-band

X-ray photoelectron spectroscopy (XPS)

XPS was performed on a MultiLab 2000 (ThermoFisher Scientific), utilizing a monochromatic Al Kα X-ray source (1486.6 eV) and a hemispherical energy analyzer (Thermo Fisher Scientific, Alpha 110).
The XPS survey spectra for NTP and NTP-RT, with the analyzed stochiometric percentage of Na, Ti, P and O, are shown in **Figure S5a** and **b**, respectively. The higher stochiometric amount of titanium (8 vs. 6 %) and oxygen (69 vs. 66 %) leads to the conclusion that more TiO_2 is present in the NTP-RT sample compared to the NTP sample.

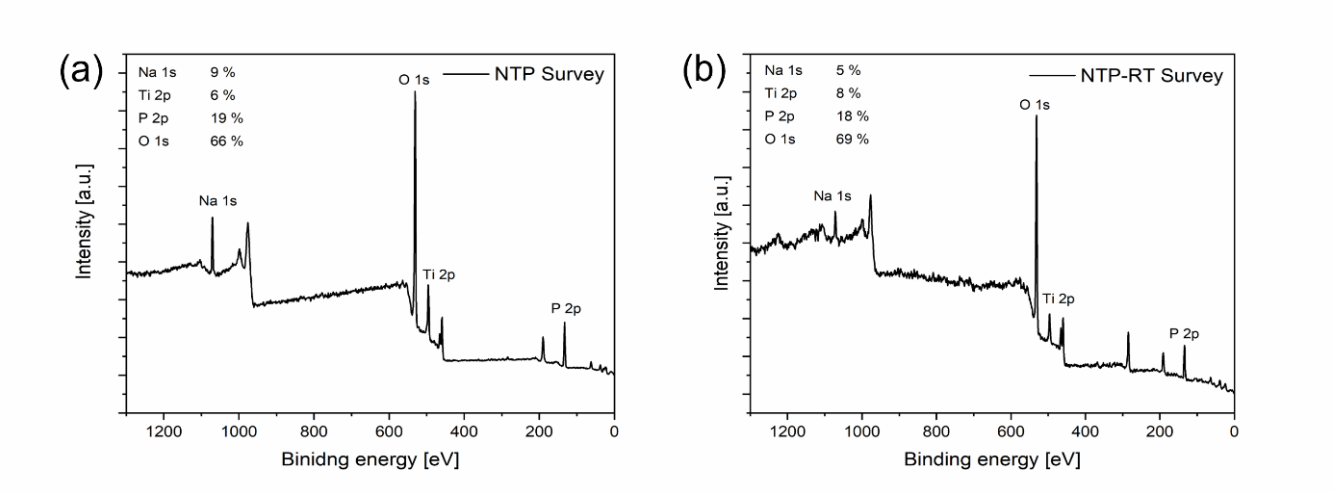

Figure S6. XPS survey spectra for a) NTP and b) NTP-RT.

Thermogravimetric Analysis (TGA)

TGA Analysis was carried out for NTP-RT using a simultaneous thermal analyser NETZSCH STA 449 F3 Jupiter.

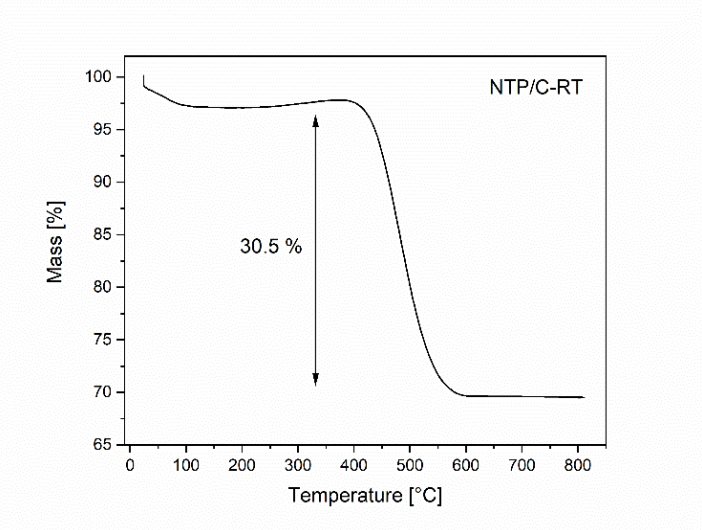

Figure S7. TGA Analysis of NTP/C-RT with a weight loss of 30.5 %.

NTP/C-RT shows a weight loss of 30.5 % at a temperature range of 400 to 600 °C. Therefore, a carbon content of 30.5 % was determined.